Treadmilling stability of a one dimensional actin growth model

Rohan C. Abeyaratne[a,*], Eric Puntel[b], Giuseppe Tomassetti[c]

[a] *Department of Mechanical Engineering, Massachusetts Institute of Technology, Cambridge, MA, USA*
[b] *Dipartimento Politecnico di Ingegneria e Architettura, Università di Udine, via del Cotonificio 114, Udine I-33100, Italy*
[c] *Dipartimento di Ingegneria, Università degli Studi Roma Tre, via Volterra 62, Roma I-00146, Italy*

Abstract

Actin growth is a fundamental biophysical process and it is, at the same time, a prototypical example of diffusion-mediated surface growth. We formulate a coupled chemo-mechanical, one-dimensional growth model encompassing both material accretion and ablation. A rod-like element composed of actin monomers is fixed at one end and connected to an elastic device at the other. The mechanical behaviour of the rod, the diffusion of free actin monomers in a surrounding solvent and the kinetic growth laws at the accreting/ablating ends are accounted for. The constitutive behaviour of actin is prescribed in fairly general terms by mainly requiring that the elastic strain energy density of the material be convex. The existence of treadmilling solutions, characterized by a constant length of the continuously evolving body, is investigated. It is shown that the present model admits at most one such solution and that it is always stable.

Keywords: actin, treadmilling, stability, surface growth

sec:intro

1. Introduction

It is well known that growth in living systems is not only promoted by biological and chemical signals but results as well from mechanical stimuli (Goriely, 2017).

Modelling growth, intended as variation of mass, poses a number of challenges in mechanics which are still being actively investigated. Among them is surface growth or accretion which, following the work of Skalak and others (Skalak et al., 1982, 1997), requires to define and track in time an ever changing, usually stress-free, reference configuration, i.e. collection of material points. The

*Corresponding Author.
Email addresses: rohan@mit.edu (Rohan C. Abeyaratne), eric.puntel@uniud.it (Eric Puntel), giuseppe.tomassetti@uniroma3.it (Giuseppe Tomassetti)

phenomenon of accretion of a solid on its boundary, occurs in several contexts of physical, technological, and biological interest. One of the most common examples of surface growth is the solidification of water at the ice-water interface near the freezing temperature; other examples include technological processes such as chemical vapor deposition and 3D printing, layered building (Bacigalupo and Gambarotta, 2012; Zurlo and Truskinovsky, 2017, 2018); in biology, the growth of hard tissues like bones and teeth (Ciarletta et al., 2013; Ganghoffer and Goda, 2018).

A second delicate issue regards the prescription of a growth law. One may simply assume that as given. Conversely, growth speed could be obtained as a result of mechanical and biochemical local conditions. These in turn may be expressed by a suitable kinetic law once the thermodynamical force driving growth is consistently defined (Abeyaratne and Knowles, 1990; Tomassetti et al., 2016).

Third, one may also describe the transport of free particles providing the material constituents for growth. In this way essential features of growth may emerge from the balance of tied mechanical and biochemical responses.

In this work we precisely analyze a one dimensional model featuring the three aforementioned characteristics, albeit in a simplified manner. We consider an elastic rod fixed at one end and connected to an elastic device at the other. The rod can grow by attaching or detaching its constituting particles (or monomers), at either end. The diffusion of free particles in a surrounding or permeating solvent and the kinetic condition for growth are accounted for. The first objective of this model is to investigate a basic reference template of chemo-mechanical growth which allows to discuss more easily modelling choices, notions and solutions.

The second motivation for this study is provided by a specific biological example, namely the growth of actin filaments. Actin in its polymerized network-forming state is an essential constituent of the cytoskeleton and is involved in cell contraction, division, motility. It is intensely studied in the bio-physical literature. See e.g. Prost et al. (2015) for a review on the physics of active gels like actin, the Ph.D. thesis of Zimmermann (2014) for a review of quantitative models of actin-based motility, and Bindschadler et al. (2004) and Cardamone et al. (2011) for just two of the many examples of different biophysical and computational models of the properties of actin networks. Pertinent to this study, but not including mechanical aspects, is a one-dimensional mathematical model of actin polymerization kinetics by Edelstein-Keshet and Ermentrout (2000).

There are interesting experimental studies (Parekh et al., 2005; Chaudhuri et al., 2007; Bieling et al., 2016) which have a setup similar to the one considered herein: an actin network is grown on a surface below the cantilever tip of an atomic force microscope (AFM) thus realizing a rod-like structure fixed at one end and restrained by an elastic device at the other. Among other things, these experiments consistently suggest that the actin network adapts to higher values of applied compressive force by correspondingly increasing its density and stiffness. This is a feature that is currently not included in our model, but it constitutes a possible refinement for future work.

Actin filaments exhibit a peculiar growth mode called treadmilling in which the length of the filament remains constant while accreting (i.e. adding) actin monomers at one end and ablating (i.e. shedding) them at the other at equal rates (see e.g. Theriot, 2000). This energy dissipating state is made possible by the hydrolysis of ATP (adenosine triphosphate) bound to actin monomers into an ADP (adenosine diphosphate) molecule and a phosphate. Despite its peculiarity, treadmilling may also be seen as a specific instance of a more common biological paradigm by which systems, tissues or organisms continuously substitute their constituents or cells at specific rates even when their overall size is no longer changing.

This work has two main results. First, under general assumptions on the behaviour of the material constituting the rod, it is possible to prove the existence of at most one treadmilling state.

Secondly the stability of such solution is discussed. Herein stability is not addressed geometrically in classical structural mechanics terms (i.e. buckling), but it is instead asked whether perturbations of the treadmilling state may cause the rod to abandon indefinitely its stationary length. It is found that in the latter sense the treadmilling solution is always stable whenever it exists.

These results may hopefully constitute a useful term of comparison and interpretative tool for other more complex models and experiments. For instance, the latter one concerning stability of treadmilling solutions may provide clarification or further evidence in support of the "emergence of a universal growth path" observed in a similar context by Abi-Akl et al. (2018) in a forthcoming paper.

The discussion on stability of the solution has also been motivated by experiments studying the growth and relative stability of an annulus of actin accreting on the surface of a spherical bead (Cameron et al., 1999; Noireaux et al., 2000; van der Gucht et al., 2005). These experiments where in turn inspired by bacterium Listeria monocytogenes which exploits cytoplasmic actin to form a polymerized tail and move out of the cell membrane and spread (Prost et al., 2008). Existing numerical and modelling efforts on this subject can be found in (John et al., 2008; de Buyl et al., 2013).

A model for a spherical annulus of actin growing on the surface of a sphere was formulated by Tomassetti et al. (2016). Therein the treadmilling solutions were characterized as well. A planned continuation of the above study and of the present one is the analysis of stability of the treadmilling solutions of that system.

The article is structured as follows. Section 2 describes the one-dimensional model in its mechanical, chemical and growth aspects. Section 3 provides the material constitutive description of the rod while the derivation of the kinetic laws is given in Section 4. The system is reduced to a differential algebraic equation in Section 5, a form suitable for the discussion concerning the existence and stability of treadmilling solutions carried out in Section 6. Conclusive remarks are made in Section 7.

To finish the introduction I need to add some discussion of the literature. I also want to properly cite the previous work by Tomassetti et al. To be done

after the introduction:

- Derive the kinetic relationships
- Compute the force velocity relationship and see whether it is possible to perform any comparison with experiments (should we also discuss the constant force case in this regard as done by a number of authors?)
- See if we can claim global stability of the treadmilling solution and connect it with Cohen and Abi Akl's result.
- Plan the figures for each section
- Write section together with accompanying figures

sec:model

2. One-dimensional model

subsec:set

2.1. Problem setting

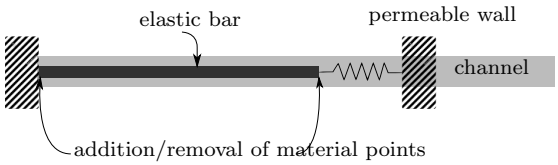

Figure 1: An elastic bar clamped between a hard and a soft device, immersed in a semi-infinite channel. to be redrawn

fig:01

We consider a one dimensional body, represented by a bar in Figure 1, which grows and deforms in a one dimensional physical space.

The bar has a natural reference configuration that occupies the segment $(x_0(t), x_1(t))$ and whose generic point is denoted by x . Here and in the following subscripts 0 and 1 refer to the left and right end sections of the bar respectively, both in the reference and in the current configuration.

As represented in Figure 2, the body is mapped in the physical one dimensional space through the function $y(x,t)$ where it occupies the segment $(y_0(t), y_1(t))$. Here and in the following shorthand notation

$$f_\alpha(t) = f(x_\alpha(t), t) \qquad \text{with } \alpha = 0, 1\ , \tag{1}$$

eq:fam

indicates in general the value of a material quantity at the end sections of the reference configuration. In particular $y_0(t)$ and $y_1(t)$ simply indicate the position of the end sections of the bar in the current configuration.

In regard to constraints, the terminal side x_0 of the bar is attached to the point Y_0 in the physical space, so that $y_0 = y(x_0(t), t) = Y_0$. Conversely, the terminal side x_1 is attached to one end of a linear spring of stiffness K. The rest position of this end of the spring is Y_1. Its other end is fixed.

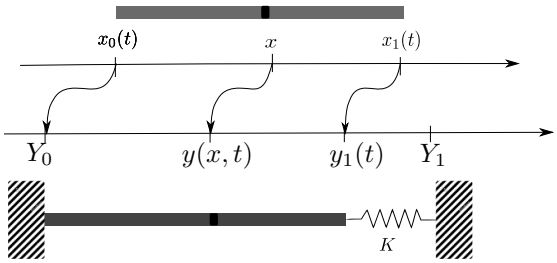

Figure 2: Reference (top) and current (bottom) configuration of the elastic bar. to be redrawn fig:02

The bar is made of molecules, hereafter called *monomers*, which are in a bound, polymerized state. The same monomers in a free, unbound state are in solution in the solvent which fills a one dimensional infinite channel, depicted with a gray-shaded rectangle in Figure 1. Free monomers flow in the interval $(y_0(t), y_1(t)) = (Y_0, y_1(t))$ according to Fick's law. We can think of them either flowing only through the bar or flowing as well through the portion of the channel not occupied by the bar. They can freely cross the point y_1, where the body is in contact with a reservoir of monomers, but cannot flow past the left support Y_0 which is assumed to be impermeable. The chemical potential of free monomers at $y_1(t)$ is held fixed and equal to μ_1, and there is an infinite supply of monomers at y_1.

Finally, under suitable growth conditions to be later specified, free monomers may accrete, i.e. attach, at either end of the bar and conversely, bound monomers occupying the end positions x_0 and x_1 of the bar may ablate, i.e. detach, and return to their free state. When accretion or ablation occur, the referential points x_0 and x_1, and hence the reference length of the bar, can change.

We now specify the equations governing the system just described.

subsec:mech

2.2. Mechanics

We require the deformation mapping $y(x) : x \to y$ to be one to one by prescribing that the stretch $\lambda = y' = \partial y/\partial x$ be positive:

$$\lambda(x,t) = y'(x,t) > 0 \ .$$

Here and in the following we use the prime to denote the derivative with respect to variables other than time for functions of one variable other than time or for functions of time and of an additional variable. That is $f' = \partial f/\partial \bullet$ with $f = f(\bullet)$ or $f = f(\bullet, t)$ with t indicating time and $\bullet \neq t$. The dot is used, as customary, to indicate partial derivative with respect to time, i.e. $\dot{f} = \partial f/\partial t$.

We do not specify a constitutive law for the bar. We simply assume the material to be hyperelastic and therefore characterized by a strain energy density $W(\lambda)$ from which we can compute the axial force σ in the bar as

$$\sigma(x,t) = W'(\lambda(x,t)) \ .$$

A number of additional assumptions on the strain energy density are detailed in Section 3.1. Given that W does not depend explicitly on x, it is anyway already evident that the material constituting the bar is also homogeneous.

eq:mech

The mechanical model for the bar is summarized in the set of equations (2) below.

$$\begin{cases} \dfrac{\partial \sigma}{\partial x} = 0 & \text{in } (x_0(t), x_1(t)), \quad (2a) \quad \texttt{eq:mech1} \\ \sigma = W'(\lambda), \quad \lambda = y' & \text{in } (x_0(t), x_1(t)), \quad (2b) \quad \texttt{eq:mech2} \\ y_0(t) = y(x_0(t), t) = Y_0 & \text{in } x_0(t), \quad (2c) \quad \texttt{eq:mech3} \\ \sigma_1(t) + K(y_1(t) - Y_1) = 0 & \text{in } x_1(t)\ . \quad (2d) \quad \texttt{eq:mech4} \end{cases}$$

Equation (2a) represents the local equilibrium in the reference configuration and it implies that the axial force is constant in x. In eq. (2b) we find again the constitutive law and the definition of the stretch. Being σ constant in x, we obtain that λ is constant as well in x and that y is linear in x.

The boundary condition prescribing that the leftmost section of the bar is fixed in $y = Y_0$ is expressed in eq. (2c). The axial force $\sigma_1(t) = \sigma(x_1(t), t)$ in $x = x_1(t)$ is prescribed by the elongation of the spring of stiffness K in eq. (2d). Again, given that σ is independent of x, (2d) actually prescribes the value of the axial force in the whole bar.

subsec:diff

2.3. Diffusion

eq:diff

The following system

$$\begin{cases} \dfrac{\partial h}{\partial y} = 0 & \text{in } (Y_0, y_1(t)), \quad (3a) \quad \texttt{eq:diff1} \\ h + m\mu' = 0 & \text{in } (Y_0, y_1(t)), \quad (3b) \quad \texttt{eq:diff2} \\ h(y_0(t), t) = h(Y_0, t) = \varrho \dot{x}_0(t) & \text{in } Y_0, \quad (3c) \quad \texttt{eq:diff3} \\ \mu(y_1(t), t) = M_1 & \text{in } y_1(t)\ . \quad (3d) \quad \texttt{eq:diff4} \end{cases}$$

governs the flux $h(y, t)$ in the positive y direction and the chemical potential $\mu(y, t)$ of monomers flowing with mobility m through the bar. The first equation (3a) expresses the conservation of mass. In it we have omitted a term $\partial h/\partial t$ by assuming that diffusion is much faster than growth. Flux has the dimension of moles per unit time. The second equation (3b) represents Fick's law. The third equation (3c), a boundary balance of mass, states that the flux of monomers at the impermeable wall is equal to the amount of monomers that detach from the left endpoint of the bar per unit time, which in turn is proportional to the ablation velocity $\dot{x}_0$ through a constant ϱ. We think of ϱ as the number of moles of bound actin monomer per unit length in the reference configuration. The fourth equation (3d) expresses the condition of chemical equilibrium at the rightmost point of the bar through a constant, assigned value M_1 of the chemical potential $\mu(y_1(t), t)$.

subsec:accr

2.4. Accretion

As anticipated in the Introduction, a key ingredient of this model is the growth law governing the evolution of the referential configuration of the bar. We assume a simple, linear kinetic law of the form

$$B_\alpha V_\alpha = F_\alpha \qquad \text{with } \alpha = 0, 1 \tag{4}$$

eq:kinshort

realistically most suitable for small deviations from thermodynamic equilibrium. In eq. (4), $\alpha = 0, 1$ denotes either end of the bar, V_α is the accretion velocity, B_α is a positive kinetic coefficient and F_α is the thermodynamical force driving accretion. The expression of F_α, derived afterwards in section 4, is

$$F_\alpha = \varrho(\mu_\alpha - M_{B,\alpha}) + W^*(\sigma_\alpha), \tag{5}$$

eq:Fa

where σ_α and μ_α are *material* descriptions of fields μ, σ evaluated at x_α and following the notation introduced in (1). Parameter $M_{B,\alpha}$ is a material constant interpreted as the chemical potential of bound monomers at x_α and $W^*(\sigma)$ is the *complementary* strain energy density whose definition and properties are given in Section 3.2. In particular in there we will see that a tensile stress $\sigma > 0$ corresponds to positive $W^*(\sigma)$ thus promoting growth according to (4)-(5). This is consistent with the layman's notion of stress induced growth popularized by images of abnormal growth of earlobes, necks and other body parts subject to sustained tension, especially observed in some indigenous tribes (see e.g. Goriely, 2017, Chapter 2.1).

Motivated by the behaviour of actin filaments, see e.g. Theriot (2000), we admit two distinct values $M_{B,0}$ and $M_{B,1}$ for the chemical potential of monomers in the bound state. Actin monomers are bound to ATP (Adenosine TriPhosphate) when they first polymerize, i.e. accrete, but after some time a hydrolysis reaction ensues by which the ATP releases a phosphate group and the polymerized actin monomer remains tied to an ADP (Adenosine DiPhosphate) molecule. The hydrolysis reaction releases energy, part of which remains stored in the polymerized actin. Therefore ADP-actin is at a higher energy level, i.e. chemical potential, than ATP-actin. Due to differences in the properties of opposite ends of actin filaments, respectively called "barbed" and "pointed", the former is usually occupied by a lower-energy ATP-actin monomer and the latter by a higher energy ADP bound actin monomer. Hence the distinction between values of the chemical potential of polymerized actin $M_{B,0}$ and $M_{B,1}$ at the two ends of the bar.

Recognizing that a positive accretion velocity corresponds to a negative rate $\dot{x}_0$ and to a positive rate $\dot{x}_1$, and reminding that we are using the notation of equation (1), the specialization of (4) and (5) to the two ends of the bar can be written as

eq:accr

$$\begin{cases} -B_0\dot{x}_0(t) = \varrho(\mu_0 - M_{B,0}) + W^*(\sigma_0(t)), & \text{in } x_0(t), \qquad (6a) \quad \texttt{eq:accr1} \\ B_1\dot{x}_1(t) = \varrho(\mu_1 - M_{B,1}) + W^*(\sigma_1(t)) & \text{in } x_1(t). \qquad (6b) \quad \texttt{eq:accr2} \end{cases}$$

Despite the simplicity of the one dimensional model, the above equations allow to close the feedback loop between stress and growth. On the one hand in fact,

the presence of the spring in (2) allows growth to affect stress, while on the other hand, growth rates in (6) are influenced by stress.

The evolution equations (6) also provide closure for the boundary-value problem (2) and (3). In fact, the solution of (2)–(3) depends only on the instantaneous values of $x_0(t)$, $x_1(t)$ and of the rate $\dot{x}_0(t)$. This means, in particular, that the right-hand sides of the equations (6) ultimately depend only on $x_0(t)$, $x_1(t)$ and $\dot{x}_0$. We therefore conclude that the combination of (2), (3), and (6) is equivalent to a first-order system in the unknowns $x_0(t)$ and $x_1(t)$. As such, this system must be complemented by initial conditions

$$x_0(0) = x_{00}, \qquad x_1(0) = x_{10} \quad \text{and} \quad y_1(0) = Y_{10}. \tag{7}$$ eq:xyinit

sec:const

3. Constitutive behaviour

We assume the bar to be made of a homogeneous, hyperelastic material and we define its constitutive behaviour through the strain energy density function $W(\lambda)$. As seen in equation (2b), the stress σ is given by $W'(\lambda)$ while $W''(\lambda)$ represents the tangent stiffness.

subsec:W

3.1. Strain energy density

eq:Wass

A specific expression for $W(\lambda)$ is not prescribed. Instead, strain energy density is characterized by a set of assumptions which are listed below

$$\begin{cases} W(1) = 0 & & \text{(8a)} & \texttt{eq:Wass1} \\ W'(1) = 0 & & \text{(8b)} & \texttt{eq:Wass2} \\ W(\lambda) \to +\infty & \text{as } \lambda \to 0^+ & \text{(8c)} & \texttt{eq:Wass3} \\ W(\lambda) \to +\infty & \text{as } \lambda \to +\infty & \text{(8d)} & \texttt{eq:Wass4} \\ W'(\lambda) \to +\infty & \text{as } \lambda \to +\infty & \text{(8e)} & \texttt{eq:Wass5} \\ W''(\lambda) > 0 & \forall \lambda > 0 & \text{(8f)} & \texttt{eq:Wass6} \end{cases}$$

and discussed in the following.

The strain energy density is defined but for an arbitrary constant which is conveniently set in (8a) by assigning zero energy to the undeformed case in which the stretch λ is equal to 1. In this latter case the stress σ is also zero as prescribed by eq. (8b). Equations (8c) and (8d) express the requirement that infinite strain energy is necessary to, respectively, infinitely compress and infinitely extend the material the bar is made of. Probably the strongest condition on $W(\lambda)$ is given by eq. (8f) which enforces convexity of the strain energy which in turn means that the tangent stiffness is positive everywhere, i.e. there are no stress softening branches under increasing stretch. Assuming sufficient regularity of $W(\lambda)$, equations (8c) and (8f) can be used to prove that, when the stretch tends to zero, the stress tends to infinity, that is $\sigma \to -\infty$ when $\lambda \to 0^+$. It is easy to see that conditions (8d) and (8f) are not sufficient to obtain an analogous result for the case in which the stretch tends to infinity. The condition that $\sigma \to +\infty$

when $\lambda \to +\infty$ is therefore explicitly given in (8e). We note in passing that the set of assumptions (8) is introduced in a constructive way and is not minimal since (8d) follows from (8e) and (8f).

From the properties of $W(\lambda)$ ensue those of the stress σ. Let

$$\widehat{\sigma}(\lambda) := W'(\lambda) \quad , \quad \widehat{\sigma}(\lambda) : \mathbb{R}^+ \longrightarrow \mathbb{R} \, , \tag{9}$$

eq:shat

then from (8f) we know that $\widehat{\sigma}$ is monotonically increasing and, taking into account (8c)-(8e) as well, that it spans the whole real line.

The stress $\widehat{\sigma}$ as a function of the stretch is therefore invertible and function

$$\widehat{\lambda}(\sigma) : \mathbb{R} \longrightarrow \mathbb{R}^+ \, , \quad \widehat{\lambda}(\sigma) \text{ such that } W'(\widehat{\lambda}) = \sigma \tag{10}$$

eq:lhat

is uniquely defined. It can be easily seen that $\widehat{\lambda}(\sigma)$ is monotonically increasing

$$\widehat{\lambda}'(\sigma) = \frac{1}{W''(\lambda)} > 0 \tag{11}$$

eq:lhat'

and that it possesses the following properties

$$\widehat{\lambda}(\sigma) \to 0^+ \text{ as } \sigma \to -\infty, \qquad \widehat{\lambda}(0) = 1, \qquad \widehat{\lambda}(\sigma) \to +\infty \text{ as } \sigma \to +\infty. \tag{12}$$

eq:lhatprop

subsec:W*

3.2. Complementary strain energy density

The complementary strain energy density $W^*(\sigma)$ is the Legendre transform of $W(\lambda)$. It defined as

$$W^*(\sigma) = \sigma\widehat{\lambda}(\sigma) - W(\widehat{\lambda}(\sigma)) \, , \tag{13}$$

eq:W*def

eq:W*

and has the properties

$$\begin{cases} W^{*\prime}(\sigma) = \lambda > 0 & \text{with } \lambda = \widehat{\lambda}(\sigma) \quad (14a) \quad \texttt{eq:W*1} \\ W^{*\prime\prime}(\sigma) = \widehat{\lambda}'(\sigma) > 0 & \forall \sigma \in \mathbb{R} \quad (14b) \quad \texttt{eq:W*2} \\ W^{*\prime}(\sigma) \to 0^+ & \text{as } \sigma \to -\infty \quad (14c) \quad \texttt{eq:W*3} \\ W^{*\prime}(\sigma) \to +\infty & \text{as } \sigma \to +\infty \quad (14d) \quad \texttt{eq:W*4} \\ W^*(0) = 0 & \quad (14e) \quad \texttt{eq:W*5} \\ W^*(\sigma) \to \pm\infty & \text{as } \sigma \to \pm\infty \quad (14f) \quad \texttt{eq:W*6} \end{cases}$$

The defining property of $W^*(\sigma)$ is (14a). It ensues from the definition (13),

$$W^{*\prime}(\sigma) = \widehat{\lambda}(\sigma) + \sigma\widehat{\lambda}'(\sigma) - W'(\lambda)\widehat{\lambda}'(\sigma) = \widehat{\lambda}(\sigma) \, .$$

Given that λ is always positive, we have that $W^*(\sigma)$ is a monotonically increasing function. Moreover, by further derivation and by (11), we obtain, see (14b), that $W^*(\sigma)$ is also strictly convex. Properties (14c) and (14d) are simply restatements of (12). Property (14e) follows from the definition of $W^*(\sigma)$ and, together with monotonicity, implies that $W^*(\sigma) > 0$ when $\sigma > 0$ and $W^*(\sigma) < 0$ when $\sigma < 0$. The last property (14f) follows as well from the definition and the preceding properties. It is important because it implies that $W^*(\sigma) : \mathbb{R} \longrightarrow \mathbb{R}$ is surjective, and given the injectivity implied by (14a), also invertible. We will use this result in the following, so it is worth noticing that it follows in particular from assumptions (8c) and (8e).

subsec:Wex

3.3. Examples of strain energy densities

We provide here a couple of instances of strain energy densities satisfying the requirements in eq. (8). We add also some remarks on the asymptotic growth of the constitutive laws $\widehat{\sigma}(\lambda)$ and complementary strain energy densities W^* ensuing from choices of the asymptotic dominant term of the strain energy density W.

A rational function

First let's consider an example of a rational strain energy density:

$$W(\lambda) = \frac{EA}{6}(\lambda^2 + 2\lambda^{-1} - 3)\,, \tag{15}$$

eq:Wex1

whence $\sigma = W'(\lambda) = \frac{EA}{3}(\lambda - \lambda^{-2})$ and $W''(\lambda) = \frac{EA}{3}(1 + 2\lambda^{-3})$. Notice that $W''(1) = EA$ and that this W obeys all assumptions in (8). Then W^* can be obtained,

$$W^* = \frac{EA}{6}\left[\lambda^2 - 4\lambda^{-1} + 3\right]\Big|_{\lambda=\widehat{\lambda}(\sigma)}\,,$$

together with its derivatives,

$$W^*(\sigma) = \lambda\Big|_{\lambda=\widehat{\lambda}(\sigma)} > 0 \quad \text{and} \quad W^{*\,\prime\prime}(\sigma) = \frac{3}{EA(1+2\lambda^{-3})}\Big|_{\lambda=\widehat{\lambda}(\sigma)} > 0\,.$$

The closed form expression of W^* is lengthy, but we can easily look at its asymptotic behaviour when $\sigma \to \pm\infty$

$$W^* \sim \frac{3}{2}\frac{\sigma^2}{EA} \to \infty \quad \text{for } \sigma \to \infty, \qquad W^* \sim \sqrt{\frac{4}{3}EA}\,\sqrt{-\sigma} \to -\infty \quad \text{for } \sigma \to -\infty$$

More generally, suppose

$$W(\lambda) \sim \alpha\lambda^n, \qquad \sigma \sim \alpha n\lambda^{n-1}, \qquad \alpha > 0, n > 1, \qquad \text{as } \lambda \to \infty.$$

Then

$$\lambda \sim \left(\frac{\sigma}{\alpha n}\right)^{\frac{1}{n-1}}, \qquad W^* \sim \alpha(n-1)\left(\frac{\sigma}{\alpha n}\right)^{\frac{n}{n-1}} \to \infty \qquad \text{as } \sigma \to \infty.$$

Similarly suppose

$$W(\lambda) \sim \beta\lambda^{-m}, \qquad \sigma \sim -\beta m\lambda^{-m-1}, \qquad \beta > 0, m > 0, \qquad \text{as } \lambda \to 0.$$

Then

$$\lambda \sim \left(\frac{\beta m}{-\sigma}\right)^{\frac{1}{m+1}}, \qquad W^* \sim -\beta(m+1)\left(\frac{-\sigma}{\beta m}\right)^{\frac{m}{m+1}} \to -\infty \qquad \text{as } \sigma \to -\infty$$

Example 2:

$$W(\lambda) = \frac{EA}{2}\left(\frac{\lambda^2}{2} - \ln\lambda - \frac{1}{2}\right)$$

$$\sigma = W'(\lambda) = \frac{EA}{2}\left(\lambda - \lambda^{-1}\right)$$
$$\lambda = \widehat{\lambda}(\sigma) = \frac{1}{EA}\left[\sigma + \sqrt{\sigma^2 + (EA)^2}\right]$$
$$W^*(\sigma) = \frac{EA}{2}\left(\frac{\lambda^2}{2} + \ln\lambda - \frac{1}{2}\right)$$

sec:kinder

4. Derivation of the kinetic laws

Accretion is a non-equilibrium process involving dissipation. The latter can be computed as the product of a flux, accretion rates in our case, and of a conjugate driving force which quantifies the departure from thermodynamic equilibrium.

In this section we provide the derivation of the expression of the driving force in eq. (5). We follow Tomassetti et al. (2016) and Abeyaratne and Knowles (1990, 1997).

We start from the expression of the dissipation rate,

$$\text{dissipation rate} = \sigma\frac{dy}{dt}\Big|_{x_0}^{x_1} + \varrho(\mu - M_B)\dot{x}\Big|_{x_0}^{x_1} - \frac{d}{dt}\int_{x_0}^{x_1} W(\lambda)dx\,, \tag{16}$$

eq:dissdef

which is given by the sum of three terms. The first represents the mechanical power of external loads, the second the inflow of chemical energy per unit time and the third the energy flow per unit time elastically stored in the material and therefore not dissipated.

We observe that the velocity of a point on the boundary

$$\frac{d}{dt}y(x(t),t) = \dot{y} + y'\dot{x} = \dot{y} + \lambda\dot{x} \tag{17}$$

eq:vel

is given by the sum of the velocity of a material point sitting at the boundary in the current instant and of the velocity of the boundary.

We rewrite the third term in (16) using divergence and transport theorems and equations (2a) and (2b),

$$\begin{aligned}\frac{d}{dt}\int_{x_0}^{x_1} W(\lambda)dx &= \int_{x_0}^{x_1} W'(\lambda)(\dot{y})'dx + W(\lambda)\dot{x}\Big|_{x_0}^{x_1}\\ &= (\sigma\dot{y} + W(\lambda))\dot{x}\Big|_{x_0}^{x_1}\,.\end{aligned} \tag{18}$$

eq:Wdiv

Substituting equations (17) and (18) into the expression (16) of the dissipation rate we obtain

$$\begin{aligned}\text{dissipation rate} &= (\sigma\dot{y} + \sigma\lambda\dot{x} + \varrho(\mu - M_B)\dot{x} - (\sigma\dot{y} + W(\lambda))\dot{x})\Big|_{x_0}^{x_1}\\ &= (\varrho(\mu - M_B) + (\sigma\lambda - W(\lambda)))\,\dot{x}\Big|_{x_0}^{x_1}\\ &= (\varrho(\mu - M_B) + W^*(\sigma))\dot{x}\Big|_{x_0}^{x_1}\,,\end{aligned} \tag{19}$$

eq:diss2

in which the multiplier of the accretive flux $\dot{x}$ is precisely the driving force of growth introduce in equation (5).

sec:DAE

5. Reduction to a differential algebraic equation

Here the system of equations presented in Section 2 is reduced to a differential algebraic equation and new notation is introduced, suitable for the ensuing discussion on the existence and stability of treadmilling solutions.

subsec:DAEmech

5.1. Mechanics

Let

$$\ell(t) = x_1(t) - x_0(t) > 0\,, \tag{20}$$

eq:ell

be the length of the rod in the reference configuration. The integration of the mechanical system of equations (2) yields

eq:msol

$$\begin{cases} y(x,t) = \lambda(t)(x - x_0) + Y_0, & \forall\ x_0(t) \le x \le x_1(t) \quad (21a) \quad \texttt{eq:msol1} \\ \sigma(t) = W'(\lambda(t)) \quad (21b) \quad \texttt{eq:msol2} \\ K\lambda(t)\ell(t) = \sigma_{\max} - \sigma(t) \quad (21c) \quad \texttt{eq:msol3} \end{cases}$$

where we have termed

$$\sigma_{\max} = K(Y_1 - Y_0) \tag{22}$$

eq:smaxdef

the maximum force attainable in the rod and in the spring. In fact, given that both $\lambda > 0$ and $\ell > 0$, it follows from (21c) that

$$\sigma < \sigma_{\max}. \tag{23}$$

eq:s<smax

We consider $\sigma_{\max}$ to be an arbitrarily tunable parameter since we can imagine being able to vary the rest position Y_1 of the spring, to the right or to the left of Y_0, to attain any desired value of $\sigma_{\max}$.

From (21a) we have

$$\lambda = (y_1 - y_0)/(x_1 - x_0) = (y_1 - y_0)/\ell \qquad \Rightarrow \qquad (y_1 - y_0) = \lambda\ell \tag{24}$$

eq:lamell

and so $\lambda\ell$ denotes the length of the body in physical space.

Equations (21) describe a unique motion $y(x,t)$ and stress $\sigma(t)$ in terms of x_0, x_1. To see it, combine (21b) and (21c) to give

$$W'(\lambda) = \sigma_{\max} - K\ell\lambda \tag{25}$$

eq:lamsol

In light of the assumed properties (8) of $W(\lambda)$, it is readily shown that there exists a unique root $\lambda > 0$ of this equation corresponding to any given $\ell > 0$, $K > 0$ and $\sigma_{\max}$. The corresponding stress is then given by (21b). These representations will of course involve given values of K, Y_0, Y_1 and the yet to be found values x_0, x_1.

The length ℓ of the body in reference space given through (21c) can be expressed in terms of stress σ as

$$\ell = \bar{\ell}(\sigma) := \frac{\sigma_{\max} - \sigma}{K\widehat{\lambda}(\sigma)}, \tag{26}$$

eq:ls

where the function $\widehat{\lambda}(\sigma)$ is the inverse of the stress-stretch relation $\sigma = W'(\lambda)$ introduced in eq. (10). In view of (11)-(12), this shows that

$$\bar{\ell}'(\sigma) < 0, \quad \bar{\ell}(\sigma) \to +\infty \text{ as } \sigma \to -\infty, \quad \bar{\ell}(\sigma) \to 0^+ \text{ as } \sigma \to \sigma_{\max}^-. \tag{27}$$

eq:lsprop

The function $\bar{\sigma}(\ell)$ that is inverse to $\bar{\ell}(\sigma)$ obeys

$$\begin{aligned} &\bar{\ell}(\bar{\sigma}(\ell)) = \ell && \bar{\sigma}(\ell) \to \sigma_{\max}^- \quad \text{as } \ell \to 0^+, \\ &\bar{\sigma}'(\ell) < 0 && \bar{\sigma}(\ell) \to -\infty \quad \text{as } \ell \to +\infty \end{aligned} \tag{28}$$

eq:sl

so that in particular as the length ℓ increases, the spring is increasingly compressed and the stress σ decreases monotonically.

subsec:DAEdiff

5.2. Diffusion

eq:dsol

The solution of the system of equation (3) yields

$$\begin{cases} \mu(y,t) = M_1 \dfrac{y - y_0}{y_1 - y_0} + \mu_0 \dfrac{y_1 - y}{y_1 - y_0}, & \forall \ y_0(t) \le y \le y_1(t) \qquad (29a) \quad \texttt{eq:dsol1} \\ h(y,t) = -m \dfrac{M_1 - \mu_0}{y_1 - y_0} \qquad (29b) \quad \texttt{eq:dsol2} \\ \mu_0 = M_1 + \dfrac{\varrho}{m} (y_1 - y_0)\, \dot{x}_0 \qquad (29c) \quad \texttt{eq:dsol3} \end{cases}$$

where we recall that $y_1 - y_0 = \lambda \ell$. We use (29c) to eliminate the unknown chemical potential μ_0, then (21c),(24) to express μ_0 in terms of the force σ,

$$\mu_0 = M_1 + \frac{\varrho}{Km} (\sigma_{\max} - \sigma)\, \dot{x}_0 \,. \tag{30}$$

eq:mu0s

subsec:DAEaccr

5.3. Accretion

eq:asub

Using (30) and noting that $\sigma_0(t) = \sigma_1(t) = \sigma(t)$, we rewrite the pair of kinetic equations (6) as

$$\begin{cases} \dot{x}_0(t) = -\dfrac{1}{B_0} \dfrac{\varrho(M_1 - M_{B,0}) + W^*(\sigma(t))}{1 + \frac{\varrho^2}{mB_0K}(\sigma_{\max} - \sigma)}, \qquad (31a) \quad \texttt{eq:asub1} \\ \dot{x}_1(t) = \dfrac{1}{B_1} \left(\varrho(M_1 - M_{B,1}) + W^*(\sigma(t))\right) \qquad (31b) \quad \texttt{eq:asub2} \end{cases}$$

We now introduce forces $\sigma_{\alpha 0}$, $\sigma_{\alpha 1}$ exploiting the bijectivity of $W^*(\sigma)$ in $\mathbb{R}$

$$\sigma_{\alpha 0} \ : \ -W^*(\sigma_{\alpha 0}) = \varrho(M_1 - M_{B,0}) \,, \quad \sigma_{\alpha 1} \ : \ -W^*(\sigma_{\alpha 1}) = \varrho(M_1 - M_{B,1}) \,, \tag{32}$$

eq:salpha

and forces $\Delta\sigma$, σ_{asym}

$$\Delta\sigma \coloneqq \sigma_{\text{asym}} - \sigma_{\max} \coloneqq \frac{mB_0K}{\varrho^2} > 0 \,, \tag{33}$$

eq:sasym

eq:afin

which allow us to reach the form

$$\begin{cases} \dot{x}_0(t) = R_0(\sigma) \coloneqq -\dfrac{\Delta\sigma}{B_0}\ \dfrac{W^*(\sigma(t)) - W^*(\sigma_{\alpha 0})}{\sigma_{\text{asym}} - \sigma}, & \text{(34a)} \quad \texttt{eq:afin1} \\ \dot{x}_1(t) = R_1(\sigma) \coloneqq \dfrac{1}{B_1}\ (W^*(\sigma(t)) - W^*(\sigma_{\alpha 1})) & \text{(34b)} \quad \texttt{eq:afin2} \end{cases}$$

for the accretion rates $\dot{x}_0(t)$, $\dot{x}_1(t)$ as functions $R_0(\sigma)$ and $R_1(\sigma)$ of the force, respectively.

Notice that $\sigma_{\alpha 0}$ and $\sigma_{\alpha 1}$ represent the forces for which $\dot{x}_0(t)$, $\dot{x}_1(t)$ are zero and that, according to their definition (32), they may be changed, but not independently, varying the chemical potential of the solvent bath M_1. In addition, for the admissible values (23) of the force σ smaller than $\sigma_{\max}$, relation (33) and the monotonicity (14a) of $W^*(\sigma)$ tell us that

$$R_0(\sigma) \lesseqgtr 0 \ \text{ for } \sigma \lesseqgtr \sigma_{\alpha 0} \text{ and } \sigma < \sigma_{\max}\,, \quad R_1(\sigma) \gtreqless 0 \ \text{ for } \sigma \gtreqless \sigma_{\alpha 1}\,. \qquad (35) \quad \texttt{eq:R>0}$$

For $R_1(\sigma)$ we can also easily infer its properties from those of W^*: it is a convex, monotonic function whose image is all $\mathbb{R}$ and whose derivative tends to 0^+ for $\sigma \to -\infty$ and to $+\infty$ for $\sigma \to +\infty$.

Looking at the first derivative of $R_0(\sigma)$,

$$R_0'(\sigma) = -\frac{\Delta\sigma}{B_0}\ \frac{W^*(\sigma) - W^*(\sigma_{\alpha 0}) + W^{*\prime}(\sigma)(\sigma_{\text{asym}} - \sigma)}{(\sigma_{\text{asym}} - \sigma)^2}\,, \qquad (36) \quad \texttt{eq:R0'}$$

we observe that it is strictly negative when conditions $\sigma > \sigma_{\alpha 0}$ and $\sigma < \sigma_{\text{asym}}$ are satisfied.

subsec:DAEeq

5.4. Differential algebraic equation

The model under consideration reduces to the following differential algebraic equation

eq:lsdae

$$\begin{cases} \dot{\ell} = R_1(\sigma) - R_0(\sigma) \\ \quad = \dfrac{1}{B_1}\ (W^*(\sigma) - W^*(\sigma_{\alpha 1})) + \dfrac{\Delta\sigma}{B_0}\ \dfrac{W^*(\sigma) - W^*(\sigma_{\alpha 0})}{\sigma_{\text{asym}} - \sigma}, & \text{(37a)} \quad \texttt{eq:lsdae1} \\ \ell = \bar{\ell}(\sigma) = \dfrac{\sigma_{\max} - \sigma}{K\ W^{*\prime}(\sigma)} & \text{(37b)} \quad \texttt{eq:lsdae2} \end{cases}$$

in which $\ell(t)$ and $\sigma(t)$ are sought under initial conditions, see (7),

$$\ell(0) = x_{10} - x_{00}, \quad \sigma(0) = W'\left(\frac{Y_{10} - Y_0}{x_{10} - x_{00}}\right)\,. \qquad (38) \quad \texttt{eq:lsinit}$$

sec:treadmill

6. Existence and stability of treadmilling solutions

We assume $M_{B,0}$ to be smaller than $M_{B,1}$, i.e. the "barbed" end to be in Y_0 and the "pointed" end in y_1. From the definition (32) and from the monotonicity (14a) of W^*, it follows that

$$\sigma_{\alpha 0} < \sigma_{\alpha 1} \tag{39}$$

eq:sa0<sa1

We seek treadmilling solutions of (37) such that $\dot{\ell} = 0$, i.e. $R_0(\sigma) = R_1(\sigma)$. We distinguish two subcases and analyze them separately.

subsec:sa0>smax

6.1. $\sigma_{\alpha 0} \leq \sigma_{\max}$: *no treadmilling*

In this case we cannot have any treadmilling solutions in the range of admissible forces given by (23). In fact we have

$$\sigma < \sigma_{\max} \leq \sigma_{\alpha 0} < \sigma_{\alpha 1}\,,$$

and equation (35) tells us that $R_0(\sigma)$ is positive and $R_1(\sigma)$ negative, so they can't have the same value.

According to (37a), we have that $\dot{\ell}$ is negative, so if we start from a finite material length $x_{10} - x_{00}$, the rod progressively loses all of its monomers till it reaches $\ell = 0$ and $\sigma = \sigma_{\max}$.

subsec:sa0<smax

6.2. $\sigma_{\alpha 0} < \sigma_{\max}$: *at most one treadmilling solution*

In this case there can at most one treadmilling solution for values of σ between $\sigma_{\alpha 0}$ and $\sigma_{\alpha 1}$. In fact, according to equations (35),(36), we know that both $R_0(\sigma)$ and $R_1(\sigma)$ are negative and monotonic in that range. As shown in Figure 3, R_1 is an increasing function of σ that attains value zero in $\sigma = \sigma_{\alpha 1}$ while R_0 is a decreasing function that has value zero in $\sigma = \sigma_{\alpha 0}$. There is therefore certainly one value of force called σ_{TM} for which R_0 and R_1 have the same values and the material length ℓ of the bar is constant in time. However, for the solution to be admissible, the force σ_{TM} in the bar at treadmilling has to be smaller than $\sigma_{\max}$, see eq. (23), and this occurs if at $\sigma_{\max}$, R_0 and R_1 have already crossed, that is if

$$R_1(\sigma_{\max}) > R_0(\sigma_{\max})\,. \tag{40}$$

eq:tmcond

By substituting eq. (34) into (40) above and exploiting once again the bijectivity of W^*, we can express the condition of admissibility of the treadmilling solution as

$$\sigma_\beta < \sigma_{\max} \tag{41}$$

eq:sb<smax

where

$$\beta = \frac{B_0}{B_1} > 0 \quad \text{and} \quad \sigma_\beta \;:\; W^*(\sigma_\beta) = \frac{1}{1+\beta} W^*(\sigma_{\alpha 0}) + \frac{\beta}{1+\beta} W^*(\sigma_{\alpha 1})\,.$$

From the monotonicity of W^*, it is clear that $\sigma_{\alpha 0} < \sigma_\beta < \sigma_{\alpha 1}$. The definitions of $W^*(\sigma_{\alpha 0})$ and $W^*(\sigma_{\alpha 1})$ are in turn given in eq. (32).

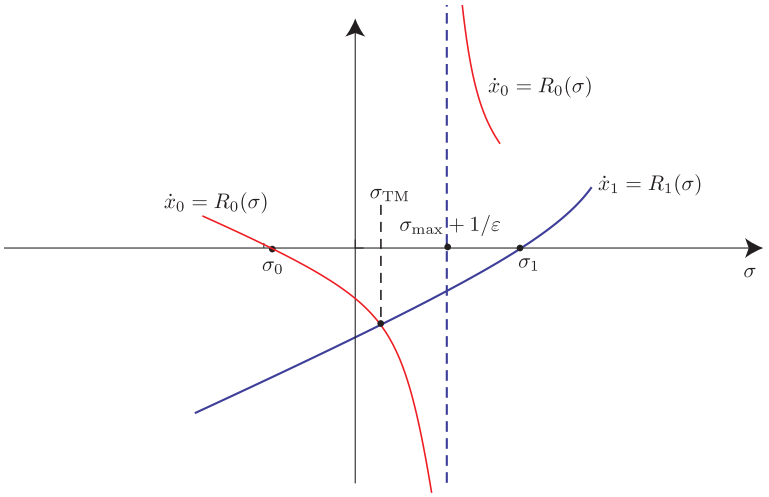

Figure 3: Graphs of $\dot{x}_0 = R_0(\sigma)$ and $\dot{x}_1 = R_1(\sigma)$. The figure has been drawn for the case $\sigma_{\rm asym} < \sigma_{\alpha 1}$ though this is not necessary. Likewise the origin need not be in the interval $(\sigma_{\alpha 0}, \sigma_{\alpha 1})$. To be redrawn. fig:tm

Thus in summary, necessary and sufficient condition for the existence of a treadmilling state under the hypothesis (39) is eq. (41). When this inequality holds, there is a unique treadmilling stress $\sigma_{\rm TM}$ at which

$$\dot{\ell} = 0 \quad \text{and} \quad \dot{x}_0 = \dot{x}_1 = R_0(\sigma_{\rm TM}) = R_1(\sigma_{\rm TM}) < 0.$$

The corresponding stretch $\lambda_{\rm TM}$ is given by $\lambda_{\rm TM} = \widehat{\lambda}(\sigma_{\rm TM})$; the growth rates at the two ends are $\dot{x}_0^{\rm TM} = \dot{x}_1^{\rm TM} = R_0(\sigma_{\rm TM}) = R_1(\sigma_{\rm TM})$; the length of the body in reference space is $\ell_{\rm TM} = (\sigma_{\rm max} - \sigma_{\rm TM})/(K\lambda_{\rm TM})$; the length of the body in physical space is $\lambda_{\rm TM}\ell_{\rm TM}$; and the chemical potential at the growing end is $\mu_0^{\rm TM} = M_1 + \varrho(\sigma_{\rm max} - \sigma_{\rm TM})\dot{x}_0^{\rm TM}/(Km)$.

6.3. Stability of treadmilling state

We now perturb the treadmilling state described in the preceding subsection. The perturbation of equation (10), $\lambda = \widehat{\lambda}(\sigma)$, yields

$$\delta\lambda = \widehat{\lambda}'(\sigma_{\rm TM})\delta\sigma$$

Operating analogously on equation (21c), $K\lambda\ell = \sigma_{\rm max} - \sigma$, gives

$$K\widehat{\lambda}(\sigma_{\rm TM})\delta\ell + K\ell_{\rm TM}\delta\lambda = -\delta\sigma$$

Combining the two preceding equations provides a relation between the perturbations $\delta\ell$ and $\delta\sigma$,

$$K\widehat{\lambda}(\sigma_{\rm TM})\,\delta\ell + \Big(K\ell_{\rm TM}\widehat{\lambda}'(\sigma_{\rm TM}) + 1\Big)\,\delta\sigma = 0. \tag{42}$$ eq:psell

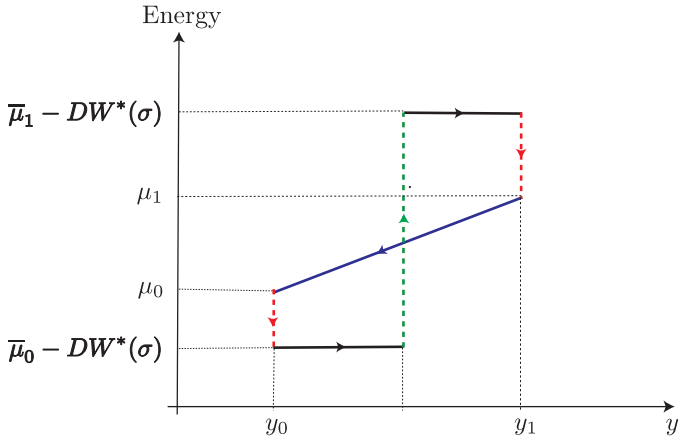

Figure 4: Energy of a monomer unit as it undergoes treadmilling. To be redrawn and described in the text.

From the expression (37a) of $\dot{\ell}(\sigma)$ we obtain

$$\delta\dot{\ell} = (R_1'(\sigma_{\rm TM}) - R_0'(\sigma_{\rm TM}))\ \delta\sigma.$$

Combining this with (42) yields

$$\delta\dot{\ell} = -F(\sigma_{\rm TM})\delta\ell \qquad \text{where} \quad F(\sigma_{\rm TM}) = \frac{R_1'(\sigma_{\rm TM}) - R_0'(\sigma_{\rm TM})}{K\ell_{\rm TM}\widehat{\lambda}'(\sigma_{\rm TM}) + 1}\, K\widehat{\lambda}(\sigma_{\rm TM}).$$

The treadmilling solution is stable if the ordinary differential equation $\delta\dot{\ell}(t) = -F(\sigma_{\rm TM})\delta\ell(t)$ has exponentially decaying solutions[1], and this occurs if and only if $F(\sigma_{\rm TM}) > 0$. Since $\widehat{\lambda}(\sigma_{\rm TM}) > 0, \ell_{\rm TM} > 0$ and $\widehat{\lambda}'(\sigma_{\rm TM}) > 0$ it follows that the treadmilling solution is stable if and only if

$$R_1'(\sigma_{\rm TM}) > R_0'(\sigma_{\rm TM}). \tag{43}$$

It is illuminating the use the monotonic relation (26) between the stress σ and the referential length ℓ to re-plot Figure 3 on the $\ell, \dot{\ell}$-plane. This effectively involves (a) reversing the direction of the σ-axis since ℓ decreases monotonically when σ increases, and (b), since $\ell = x_1 - x_0$, plotting the difference $\dot{\ell} = \dot{x}_1 - \dot{x}_0 = R_1(\sigma(\ell)) - R_0(\sigma(\ell))$ on the vertical axis. This is shown schematically in Figure 6. Observe how, if $\ell > \ell_{\rm TM}$ at some time then $\dot{\ell} < 0$ and so $\ell(t)$ will decrease until it reaches the treadmilling value $\ell_{\rm TM}$. Likewise if $\ell < \ell_{\rm TM}$, $\ell(t)$ will increase to $\ell_{\rm TM}$.

[1] If $\delta\ell(t)$ vanishes exponentially then so do the perturbations of the various other quantities.

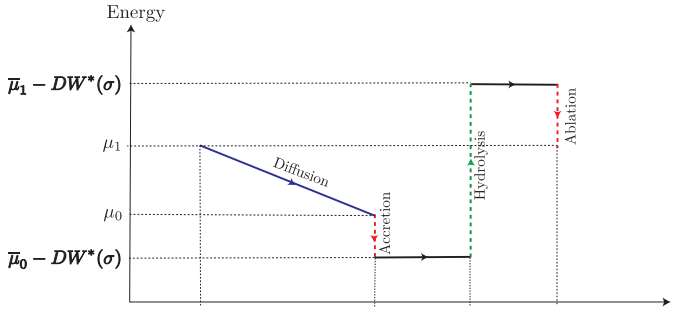

Figure 5: Energy of a monomer unit as it undergoes treadmilling.To be redrawn and described in the text.

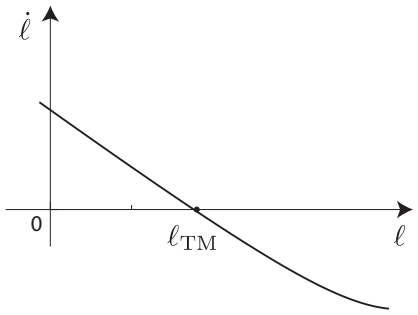

Figure 6: Graph of $\dot{\ell} = \dot{x}_1 - \dot{x}_0 = R_1(\sigma(\ell)) - R_0(\sigma(\ell))$ versus ℓ where $\sigma(\ell)$ is given through (21c).

fig:ell

sec:end

7. Conclusions

Acknowledgements

R.A. and E.P. gratefully acknowledge the support of the MIT-FVG Seed Fund. E.P. thankfully acknowledges as well the support of the Italian National Group of Mathematical Physics (GNFM-INdAM).

sec:appA

Appendix A. Examples of strain energy densities

References

AbeyaratneKnowles1990

Abeyaratne, R., Knowles, J.K., 1990. On the driving traction acting on a surface of strain discontinuity in a continuum. Journal of the Mechanics and Physics of Solids 38, 345–360. doi:10.1016/0022-5096(90)90003-M.

AbeyaratneKnowles1997 Abeyaratne, R., Knowles, J.K., 1997. A note on the driving traction acting on a propagating interface: Adiabatic and non-adiabatic processes of a continuum. Journal of Applied Mechanics 67, 829–830. doi:10.1115/1.1308577.

Abi-AklAbeyaratne:2018 Abi-Akl, R., Abeyaratne, R., Cohen, T., 2018. Kinetics of surface growth with coupled diffusion and the emergence of a universal growth path. arXiv:1803.08399v1.

BacigalupoGambarotta:2012 Bacigalupo, A., Gambarotta, L., 2012. Effects of layered accretion on the mechanics of masonry structures. Mechanics Based Design of Structures and Machines 40, 163–184. doi:10.1080/15397734.2011.628622.

BielingLi2016 Bieling, P., Li, T.D., Weichsel, J., McGorty, R., Jreij, P., Huang, B., Fletcher, D., Mullins, R.D., 2016. Force feedback controls motor activity and mechanical properties of self-assembling branched actin networks. Cell 164, 115–127. doi:10.1016/j.cell.2015.11.057.

BindschadlerOsborn2004 Bindschadler, M., Osborn, E.A., Dewey, C.F., McGrath, J.L., 2004. A mechanistic model of the actin cycle. Biophysical Journal 86, 2720–2739. doi:10.1016/S0006-3495(04)74326-X.

BuylMikhailov2013 de Buyl, P., Mikhailov, A.S., Kapral, R., 2013. Self-propulsion through symmetry breaking. EPL (Europhysics Letters) 103, 60009. doi:10.1209/0295-5075/103/60009.

CameronFooter1999 Cameron, L.A., Footer, M.J., van Oudenaarden, A., Theriot, J.A., 1999. Motility of acta protein-coated microspheres driven by actin polymerization. Proc Natl Acad Sci USA 96, 4908–4913. doi:10.1073/pnas.96.9.4908.

CardamoneLaio2011 Cardamone, L., Laio, A., Torre, V., Shahapure, R., DeSimone, A., 2011. Cytoskeletal actin networks in motile cells are critically self-organized systems synchronized by mechanical interactions. Proc Natl Acad Sci USA 108, 13978–13983. doi:10.1073/pnas.1100549108.

ChaudhuriParekh2007 Chaudhuri, O., Parekh, S.H., Fletcher, D.A., 2007. Reversible stress softening of actin networks. Nature 445, 295–298. doi:10.1038/nature05459.

CiarlettaPreziosi2013 Ciarletta, P., Preziosi, L., Maugin, G.A., 2013. Mechanobiology of interfacial growth. Journal of the Mechanics and Physics of Solids 61, 852–872. doi:10.1016/j.jmps.2012.10.011.

stein-KeshetErmentrout2000 Edelstein-Keshet, L., Ermentrout, G.B., 2000. Models for spatial polymerization dynamics of rod-like polymers. Journal of Mathematical Biology 40, 64–96. doi:10.1007/s002850050005.

GanghofferGoda2018 Ganghoffer, J.F., Goda, I., 2018. A combined accretion and surface growth model in the framework of irreversible thermodynamics. International Journal of Engineering Science 127, 53–79. doi:10.1016/j.ijengsci.2018.02.006.

Goriely:2017 Goriely, A., 2017. The Mathematics and Mechanics of Biological Growth. volume 45 of *Interdisciplinary Applied Mathematics*. 1 ed., Springer. doi:10.1007/978-0-387-87710-5.

GuchtPaluch2005 van der Gucht, J., Paluch, E., Plastino, J., Sykes, C., 2005. Stress release drives symmetry breaking for actin-based movement. Proc Natl Acad Sci USA 102, 7847. doi:10.1073/pnas.0502121102.

JohnPeyla2008 John, K., Peyla, P., Kassner, K., Prost, J., Misbah, C., 2008. Nonlinear study of symmetry breaking in actin gels: Implications for cellular motility. Physical Review Letters 100, 068101. doi:10.1103/PhysRevLett.100.068101.

NoireauxGolsteyn:2000 Noireaux, V., Golsteyn, R.M., Friederich, E., Prost, J., Antony, C., Louvard, D., Sykes, C., 2000. Growing an actin gel on spherical surfaces. Biophysical Journal 78, 1643–1654. doi:10.1016/S0006-3495(00)76716-6.

ParekhChaudhuri2005 Parekh, S.H., Chaudhuri, O., Theriot, J.A., Fletcher, D.A., 2005. Loading history determines the velocity of actin-network growth. Nature Cell Biology 7, 1219–1223. doi:10.1038/ncb1336.

ProstJuelicher2015 Prost, J., Jülicher, F., Joanny, J.F., 2015. Active gel physics. Nature Physics 11, 111–117. doi:10.1038/nphys3224.

ProstJoanny2008 Prost, J., Joanny, J.F., Lenz, P., Sykes, C., 2008. The physics of listeria propulsion, in: Lenz, P. (Ed.), Cell Motility. Springer New York, New York, NY. Biological and Medical Physics, Biomedical Engineering. chapter 1, pp. 1–30. doi:10.1007/978-0-387-73050-9_1.

SkalakDasgupta1982 Skalak, R., Dasgupta, G., Moss, M., Otten, E., Dullemeijer, P., Vilmann, H., 1982. Analytical description of growth. Journal of Theoretical Biology 94, 555–577. doi:10.1016/0022-5193(82)90301-0.

SkalakFarrow1997 Skalak, R., Farrow, D.A., Hoger, A., 1997. Kinematics of surface growth. Journal of Mathematical Biology 35, 869–907. doi:10.1007/s002850050081.

Theriot2000 Theriot, J.A., 2000. The polymerization motor. Traffic 1, 19–28. doi:10.1034/j.1600-0854.2000.010104.x.

TomassettiCohen:2016 Tomassetti, G., Cohen, T., Abeyaratne, R., 2016. Steady accretion of an elastic body on a hard spherical surface and the notion of a four-dimensional reference space. Journal of the Mechanics and Physics of Solids 96, 333–352. doi:10.1016/j.jmps.2016.05.015.

Zimmermann2014 Zimmermann, J., 2014. Modeling the lamellipodium of motile cells. Ph.D. thesis. Humboldt-Universität zu Berlin, Mathematisch-Naturwissenschaftliche Fakultät I. doi:10.18452/16871.

ZurloTruskinovsky2017 Zurlo, G., Truskinovsky, L., 2017. Printing non-euclidean solids. Physical Review Letters 119, 048001. doi:10.1103/PhysRevLett.119.048001.

ZurloTruskinovsky2018 Zurlo, G., Truskinovsky, L., 2018. Inelastic surface growth. Mechanics Research Communications 93, 174–179. doi:10.1016/j.mechrescom.2018.01.007.